Use of optically stimulated luminescence dosimeter and radiophotoliminescent glass dosimeter for dose measurement in dual-source dual-energy computed tomography

Physical and Engineering Sciences in Medicine (2021) 44:1311–1319
https://doi.org/10.1007/s13246-021-01063-6

SCIENTIFIC PAPER

Use of optically stimulated luminescence dosimeter and radiophotoliminescent glass dosimeter for dose measurement in dual-source dual-energy computed tomography

Ayaka Hirosawa[1,2] · Kosuke Matsubara[3] · Yusuke Morioka[1,2] · Masayasu Kitagawa[1,2] · Thunyarat Chusin[2,4] · Akihiro Takemura[3]

Received: 22 September 2020 / Accepted: 6 October 2021 / Published online: 19 October 2021

Abstract

We aimed to evaluate properties of optically stimulated luminescence dosimeters (OSLDs) and radiophotoluminescent glass dosimeters (RPLDs) used in dual-source dual-energy (DE) computed tomography (DECT) dosimetry. Energy dependence was evaluated in single-energy (SE) and DE modes, and their relative dose responses differed by 3.8% and 6.6% under equivalent effective energy with OSLD and RPLD, respectively. Dose variation was evaluated using coefficients of variation of dose values from 10 dosimeters, and dose variation of OSLD and RPLD in SE mode ranged from 2.1 to 3.0% and from 2.1 to 2.8%, and those in the DE mode were 1.8 and 2.6%, respectively. Dose linearity was evaluated from 1 to 150 mGy, and linear relationships of dose response were observed between the dosimeters and the ionization chamber (correlation coefficients ≥ 0.9991). Angular dependence was evaluated from $-90°$ to $+90°$, and it was smaller in DE mode than in SE mode for OSLD. The normalized response of RPLD was higher at $\pm 30°$ and $\pm 60°$ and lower at $-90°$ in SE and DE modes. This study demonstrated both OSLD and RPLD can perform dosimetry in dual-source DECT with small influence of the properties of the dosimeters compared with that in SECT.

Keywords Dual-source dual-energy computed tomography (Dual-source DECT) · Optically stimulated luminescence dosimeter (OSLD) · Radiophotoluminescent glass dosimeter (RPLD) · Dosimetry

Introduction

Computed tomography (CT) is an essential tool for protecting and improving patients' health [1]. While dual-energy (DE) CT (DECT) technology has improved recently and have been used to obtain the material decomposition of an object and to reduce metal artifacts [2–4], there are reports suggesting that the risks for radiation-induced cancer and cataracts have increased due to greater use of CT. The International Commission on Radiological Protection (ICRP) stated that, in comparison with during other radiological examinations and because of the increasing frequency of CT examinations, there is an urgent need to focus the attention of radiologists, physicians, medical physicists, and other health care personnel on the relatively higher effective doses applied during CT procedures to individual patients [5]. Considering the ICRP statement, it is increasingly critical to patient health to evaluate and minimize dose exposure in those undergoing CT examination.

✉ Kosuke Matsubara
matsuk@mhs.mp.kanazawa-u.ac.jp

1 Department of Medical Technology, Toyama Prefectural Central Hospital, 2-2-78 Nishinagae, Toyama, Toyama 930-8550, Japan

2 Department of Quantum Medical Technology, Division of Health Sciences, Graduate School of Medical Sciences, Kanazawa University, 5-11-80 Kodatsuno, Kanazawa, Ishikawa 920-0942, Japan

3 Department of Quantum Medical Technology, Faculty of Health Sciences, Institute of Medical, Pharmaceutical and Health Sciences, Kanazawa University, 5-11-80 Kodatsuno, Kanazawa, Ishikawa 920-0942, Japan

4 Department of Radiological Technology, Faculty of Allied Health Sciences, Naresuan University, Muang, Phitsanulok 65000, Thailand

Experimental dose measurements are often conducted using anatomical physical phantoms designed to allow the placement of dosimeters such as thermoluminescence dosimeters (TLDs), optically stimulated luminescence dosimeters (OSLDs) and radiophotoluminescence glass dosimeters (RPLDs) at locations corresponding to various organs, owing to the estimation of patient's organ absorbed doses being difficult because it is impossible to measure them directly [6–9]. OSLDs and RPLDs have numerous advantages as compared with TLDs [10, 11], and have been adopted as the predominant new types of luminescence dosimeters that are used for assessment purposes. The properties of these dosimeters have been evaluated for CT dosimetry [12–14]. Scarboro et al. found that OSLDs overrespond by a factor of 3.5 or more when exposed to a dose of less than 100 keV [15]. Meanwhile, Hirosawa et al. founded that RPLD with a tin filter cannot measure scattered X-ray correctly due to its poor angular dependence, and RPLD without a tin filter should be used by applied the calibration factor for CT dosimetry [14]. However, these authors' findings encompassed only those outcomes obtained using single-energy (SE) CT, and they did not perform DECT.

A dual-source CT system is equipped with two sets of X-ray tubes and detectors. These two acquisition systems are mounted onto a rotating gantry with an angular offset of 90°. When DECT is performed by using the dual-source CT system, X-rays are irradiated from two sets of X-ray tubes that are arranged in a single gantry perpendicular to each other in the X–Y plane and produce different tube voltages. To the best of our knowledge, no study has evaluated the characteristics of OSLD and RPLD for dual-source DECT in order to perform dose measurement in dual-source DECT with less uncertainty.

In this study, we evaluated the energy dependence, dose variation, dose linearity, and angular dependence of OSLD and RPLD for dose measurement in dual-source DECT. We compared the measures obtained during DECT with those obtained during single-source SECT.

Materials and methods

First, the HVLs and energy dependence of OSLD and RPLD were measured and evaluated from 70 to 150 kV at 10 kV intervals (SE mode) and three combinations of tube voltage (DE mode). Second, based on the result of the energy dependence, dose variation, dose linearity, and angular dependence of dosimeters were evaluated in SE mode and one combination of tube voltage (DE mode). The uncertainties for measurements were estimated using the methodology from ISO guide [16–18] (Table 1).

Table 1 Estimated uncertainties associated with measurement using the ISO methodology

Source of uncertainties	Type A (std unc. %)	Type B (std unc. %)
X-ray unit dose output reproducibility	1.179	
Temperature and pressure variations		0.5
Variation in response of chamber		3
Uncertainty of sensitivity for OSLD		2
Uncertainty of analyze process for OSLD		2
Variation of sensitivity for RPLD		2
Uncertainty of analyze process for RPLD		2

Std unc. standard uncertainty, *RPLD* radiophotoluminescence glass dosemeter, *OSLD* optically stimulated luminescence dosemeter

Dosimeters

A 6-cm^3 general purpose ionization chamber (model 10×5–6; Radcal, Monrovia, CA, USA) and an electrometer (model 9015; Radcal, Monrovia, CA, USA) were used with integration mode as a field dosimeter. The field dosimeter was calibrated at 70 and 120 kV beams with half-value layers (HVLs) of 3.01 and 5.23 mmAl, respectively, using a 3-cm^3 ionization chamber (DC300; Scanditronix Wellhofer, Schwarzenbruck, Germany) and an electrometer (RAMTEC-1500B; Toyo Medic, Tokyo, Japan) which were calibrated at 70 and 120 kV beams with HVLs of 3.00 and 5.00 mmAl, respectively, against a national standard dosimeter, using a radiographic X-ray generator (UD150L-RII; Shimadzu, Tokyo, Japan) in standard dosimetry facility. The calibration factor of the field dosimeter was 1.00 for both 70 and 120 kV beams with HVLs of 3.01 and 5.23 mmAl, respectively. Therefore, a calibration factor of 1.00 was adopted for all energy ranges in this study.

Two types of dosimeters, OSLD (Landauer Inc., Glenwood, IL, USA) and RPLD (AGC Techno Glass, Shizuoka, Japan), were used in this study. The numbers of used dosimeters to investigate energy dependence, dose variation, linearity, and angular dependence were 60, 40, 50, and 140, respectively.

The external dimension of the OSLD is 10×10×2 mm^3. The detector consists of a 0.2-mm-thick aluminum oxide based (Al_2O_3: C) disk shaped with a diameter of approximately 5 mm that is inserted into the plastic case. The OSLDs were initialized for 24 h under fluorescent light prior to each exposure and its signal was reduced below 100 counts by initializing. The dose values were read out within 24 h from the irradiation period and were averaged by reading each value five times on a microStar reader (Landauer Inc.) which was calibrated with a set of dedicated calibration OSLDs that the manufacturer's standard 80 kV X-ray beam with HVL of 2.9 mmAl was exposed on a PMMA phantom. The linearity correction of the reader was also performed during the calibration process. A set of dedicated OSLDs, which were irradiated with 0, 5, and 30 mGy of manufacturer's standard 80 kV X-ray beam (with HVL of 2.9 mmAl) were read three times. Based on the readout values of three different dose levels, the linearity was automatically corrected by the calibration software of the reader. Decay and counts depletion after multiple readouts were not corrected according to the white paper from Landauer [17].

RPLDs can be used with and without a tin filter. In this work, no filter was utilized as a previous study [14] found the tin filter results in poor angular dependence. The size of the RPLD is a diameter of 2.8 mm and a length of 13 mm and that of the detector is a diameter of 1.5 mm and a length of 12 mm. The RPLDs were annealed at 400ºC for 30 min prior to each exposure, while, after exposure, they were preheated at 70 °C for 30 min in order to stabilize the luminescent centers and read out within 24 h after the irradiation period using the FDG-1000 reader (AGC Techno Glass, Shizuoka, Japan), in accordance with the manufacturer's recommended protocol. The reader was calibrated with two calibration RPLDs; one was irradiated at 2 Gy to a ^{137}Cs γ-ray beam (662 keV) and another was unexposed.

CT scanner

We used a third-generation dual-source CT scanner (SOMATOM Force; Siemens Healthineers, Erlangen, Germany) to perform both SE and DE scans. The SE tube voltages ranged from 70 to 150 kV in steps of 10 kV. In DE scan, tin (Sn) prefiltration was possible to improve spectral separation, and the tube voltage pairs were 80/140, 70/Sn150, 80/Sn150, 90/Sn150, and 100/Sn150 kV, respectively. The detector A covers full scan field of view (SFOV) of 500 mm, which is the collection range of scan data, while the detector B covers smaller SFOV of 356 mm because of the space limitations in the gantry.

Energy dependence

Measurement of HVLs

We adopted the conventional non-rotating method [19]. In the SE mode, the X-ray tube was placed in the 6 o'clock direction, while the ionization chamber was placed at the isocenter of the gantry. We set the lead collimator and polystyrene foam and aluminum plates as attenuators. The integration of air kerma was measured with and without the plates in place, respectively. The measurements were also performed using the following parameters that were decided according to the previous study [19]: tube voltages of 70 to150 kV at 10 kV intervals and Sn150 kV; a tube current of 50 mA; an exposure time of 1.0 s; a detector configuration of 64 × 0.6 mm; and a SFOV of 500 mm.

In the DE mode, we set the ionization chamber, lead collimator, and polystyrene in the same geometry arrangement as the measurement in SE mode. Firstly, X-ray energy was irradiated from tube A in the 6 o'clock direction. Next, the tubes and detectors were rotated and X-ray energy was irradiated from tube B in the 6 o'clock direction. The integration of the air kerma was measured. Again, we repeated this process with and without the attenuators (plates) in place. This time, the measurements were completed using the following acquisition parameters: tube voltages of 80/Sn150, 90/Sn150, and 100/Sn150 kV, tube current combinations of 100/67 mA, 80/50 mA, and 100/50 mA; an exposure time of 1.0 s; a detector configuration of 64 × 0.6 mm; and SFOVs of 500 and 356 mm in tubes A and B, respectively. The ratios of the tube current of tubes A and B were 1:0.67, 1:0.625, and 1:0.5, respectively, according to the scanner default protocol for head CT imaging.

In both SE and DE mode, the measurements were performed three times for each thickness, and the dose values were averaged. The HVLs were calculated from the quartic approximation formulas which were delivered from the relationship between the thickness of the attenuator and obtained exposure dose for each energy levels. They were converted to effective energies using the approximate formula calculated from linear attenuation coefficient of aluminum [20].

Evaluation of energy dependence

In SE mode, the X-ray tube energy was irradiated in the 12 o'clock direction (Fig. 1). In the DE mode, the X-ray

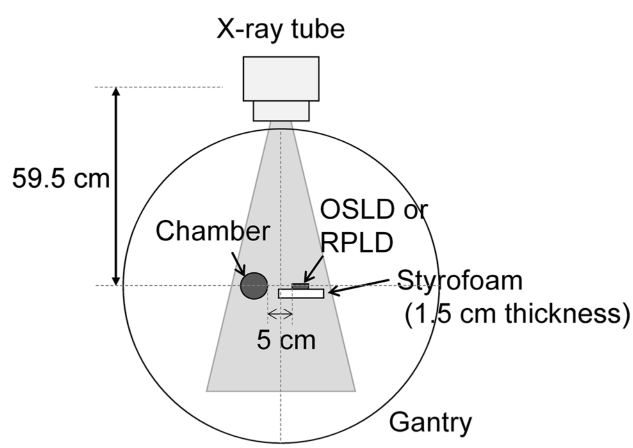

Fig. 1 Experimental setup for measuring energy dependence and dose linearity. The X-ray tube was positioned in the 12 o'clock direction. The ionization chamber and an initialized dosimeter were placed 2.5 cm from the isocenter of the gantry

energy was irradiated separately from tube A and tube B to exclude the influence of angular dependence. Firstly, the X-ray energy was irradiated from tube A in the 12 o'clock direction. Next, the X-ray energy was irradiated from tube B in the 12 o'clock direction. The dosimeters measured the integrated dose from the two X-ray tubes. The measurements were performed using the same parameters as those employed for the HVL measurement. We used one dosimeter for each measurement, measured five times, read out five times for each, then averaged 25 readings for each type of dosimeter. Energy dependence was evaluated using the following equation:

$$R = \frac{K_{air}}{K_{air,ref}}$$

where R is the relative response, K_{air} is the air kerma measured using a dosimeter, and $K_{air,ref}$ is the air kerma measured using the ionization chamber.

Dose variation

We investigated dose variation under conditions of dose measurement in CT. In SE mode, the X-ray was irradiated in the 12 o'clock direction, while an unexposed dosimeter was placed at the isocenter of the gantry. In the DE mode, the X-ray was irradiated in the 12 o'clock direction separately from tube A and tube B as well as based on the method of energy dependence. The dosimeters measured the integrated dose from both X-ray tubes. These measurements were performed using the following acquisition parameters: tube voltages of 80, 120, Sn150 kV (SE mode), or 80/Sn150 kV (DE mode); a tube current of 50 mA, an exposure time of 1.0 s; and a detector configuration of 64 × 0.6 mm; and SFOVs of 500 and 356 mm in tubes A and B, respectively. The X-ray was irradiated to 10 dosimeters separately, and each dosimeter was read out five times so that 50 readings were averaged for each type of dosimeter. The coefficients of variation were calculated using the mean and standard deviation values of dose values from 10 dosimeters adopted for each tube voltage.

Dose linearity

The geometry of measuring the dose linearity was the same as that of energy dependence (Fig. 1). In SE mode, an unexposed dosimeter and the ionization chamber were irradiated from 1 to 150 mGy based on dose measured by the ionization chamber. In the DE mode, to exclude the influence of angular dependence, an unexposed dosimeter and the ionization chamber were irradiated in the 12 o'clock direction separately from tube A and tube B as well as method of energy dependence. The dosimeters measured the integrated dose from both X-ray tubes. The measurements were performed using the following acquisition parameters: tube voltages of 120 kV (SE mode) or 80/Sn150 kV (DE mode); a tube current of 30 to 760 mA or 33/22 to 365/245 mA; an exposure time of 0.5 to 2.0 s; and a detector configuration of 64 × 0.6 mm; and SFOVs of 500 and 356 mm in tubes A and B, respectively. One dosimeter was used for each measurement. It was irradiated and read out five times repeatedly, and total 25 readings were averaged for each type of dosimeter. The averaged doses were multiplied by calibration factors which were calculated by the ratio of the dose measured by the ionization chamber to that measured by the dosimeters at 120 kV and 80/Sn150 kV with HVL of 7.83 and 8.06 mmAl, respectively. The relationship between the dose measured by the dosimeter and that measured by the ionization chamber was then evaluated.

Angular dependence

The geometry of evaluating angular dependence was the same as that employed when assessing the dose variation. In SE mode, X-ray energy was irradiated to the dosimeter from − 90° to + 90° at − 30° intervals, where 0° indicates that the X-ray was irradiated parallel along the axial direction of the RPLD and perpendicular to the OSLD from tube A, and the minus and plus symbols mean counterclockwise and clockwise, respectively (Fig. 2). In the DE mode, X-ray energy was irradiated using the different dosimeter from two tubes simultaneously. The measurements were initiated from the tube position shown in Fig. 3. They were performed using the following acquisition parameters: tube voltages of 80, 120, and Sn150 kV (SE mode) or 80/Sn150 kV (DE mode); a tube current of 50 mA; an exposure time of 1.0 s; and a detector

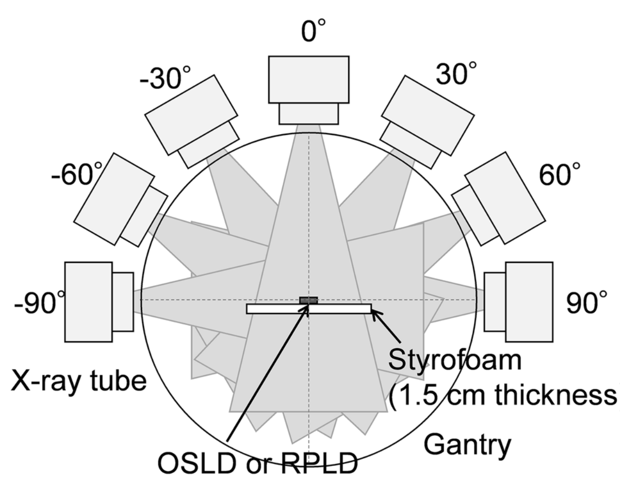

Fig. 2 Direction of the irradiated dosimeter. 90° means that the X-ray energy was irradiated parallel to the long axis of the rod

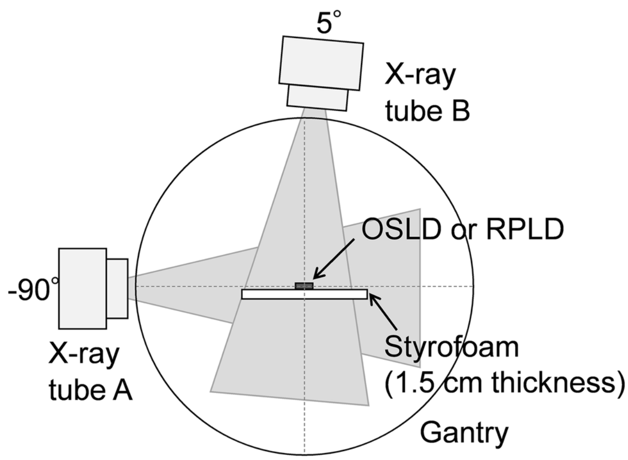

Fig. 3 Experimental setup for measuring angular dependence. The measurements were started from this tube position

configuration of 64 × 0.6 mm; and SFOVs of 500 and 356 mm in tubes A and B, respectively. We used one dosimeter for each measurement, measured five times, read out five times for each, then averaged 25 readings for each condition. The responses were normalized by the ratio of the dose at 0°.

Table 2 Half-value layers and effective energies

Tube voltage (kV)	HVL (mmAl)	Effective energy (keV)
70	4.68 ± 0.03	40.6 ± 0.1
80	5.62 ± 0.01	44.4 ± 0.0
90	6.22 ± 0.02	46.8 ± 0.0
100	6.79 ± 0.02	49.2 ± 0.1
110	7.34 ± 0.03	51.6 ± 0.1
120	7.83 ± 0.03	53.8 ± 0.1
130	8.26 ± 0.03	55.7 ± 0.1
140	8.83 ± 0.03	58.3 ± 0.1
150	9.08 ± 0.03	59.3 ± 0.1
Sn150	14.59 ± 0.03	95.4 ± 0.1
80/Sn150	8.06 ± 0.03	54.8 ± 0.1
90/Sn150	7.96 ± 0.03	54.4 ± 0.0
100/Sn150	7.94 ± 0.03	54.3 ± 0.0

HVL half-value layer

Results

Energy dependence

Measurement of HVLs

The results of the HVL and the effective energy for the tube voltages are presented in Table 2. The coefficient of variation among three measurements was 0.6% at maximum. HVLs and effective energies varied from 4.68 to 14.59 mmAl and 40.6 to 95.4 keV, respectively, in the SE mode, while they varied from 7.94 to 8.06 mmAl and 54.3 to 54.8 keV, respectively in the DE mode. The HVLs and effective energies for all DE mode were within the range of those for 120 and 130 kV in SE mode. The difference of HVL and effective energy between the DE mode was small regardless of the combination of tube voltage.

Comparison of the responses of the SE and DE modes

The relative dose responses at different HVLs for the OSLD and RPLD are included in Fig. 4. The relative dose responses compared to the ionization chamber for the OSLD and RPLD in the DE mode ranged from 0.64 ± 0.01 to 0.67 ± 0.03 and from 2.84 ± 0.08 to 2.92 ± 0.04, respectively, and the results showed that the influence of the tube voltage combination on relative dose response was small. The difference of dose response for the OSLD depending on energy was smaller than that observed for the RPLD in both the SE and DE modes. Meanwhile, the relative dose responses of the OSLD and RPLD for DE mode decreased by 3.8% and 6.6%, respectively, when compared with those for the SE mode, which was under equivalent effective energy.

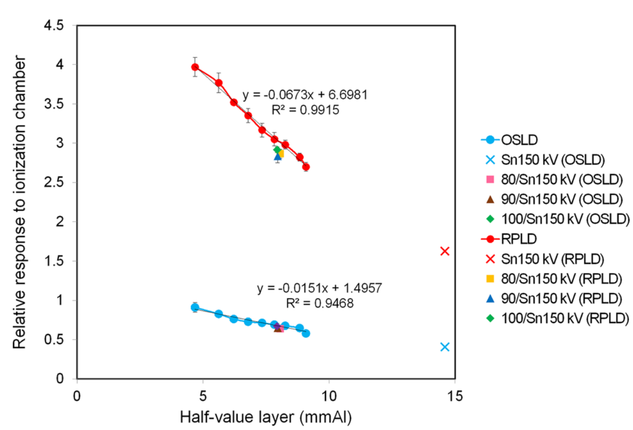

Fig. 4 Energy dependence of the relative dose response. The points show the relative dose responses compared to the ionization chamber for the OSLD and RPLD at different HVLs

Table 3 Coefficients of variation for dose response

Tube voltage (kV)	Coefficient of variance (%)	
	RPLD	OSLD
80	3.0	2.2
120	2.8	2.1
Sn150	2.1	2.8
80/Sn150	1.8	2.6

RPLD radiophotoluminescence glass dosemeter, *OSLD* optically stimulated luminescence dosemeter

Dose variation

The average coefficient of variation in the dose response is noted in Table 3. The dose variation for DE mode was evaluated with only one combination of tube voltages as the influence of the tube voltage combination of DE mode was small from the result of energy dependence. The dose variation of the OSLD in the SE mode ranged from 2.1 to 3.0% and for RPLD in the SE mode from 2.1 to 2.8%. Therefore, the dose variation of the OSLD was comparable to that of the RPLD in the SE mode. The dose variation of the OSLD and RPLD in the DE mode were 1.8 and 2.6%, respectively. It showed that the dose variation of the OSLD and RPLD in the SE mode were comparable to those in the DE mode.

Dose linearity

The dose ratios of the values measured by the dosimeter to those measured by the ionization chamber are shown in Fig. 5. When using the OSLD, there was a linear relationship observed between the dose measured by the dosimeter and that measured by the ionization chamber for both the SE and DE modes (the correlation coefficients were 0.9991 and 0.9997, respectively). Similarly, with the RPLD, there was a linear relationship between the dose measured by the dosimeter and that measured by the ionization chamber for both the SE and DE modes (the correlation coefficients were 0.9996 and 0.9999, respectively). The slope of the approximation curve for dose response between the OSLD and the ionization chamber in DE mode was larger than that in 120 kV. Conversely, the slope of the approximation curve for dose response between the RPLD and the ionization chamber in DE mode was close to that in 120 kV.

Angular dependence

The normalized dose responses from − 90° to + 90° for the OSLD and RPLD are noted in Fig. 6. The responses were averaged by the data from the five dosimeters and normalized by the ratio of the dose at 0°. The normalized dose responses by the ratio of the dose at 0° for the OSLD and

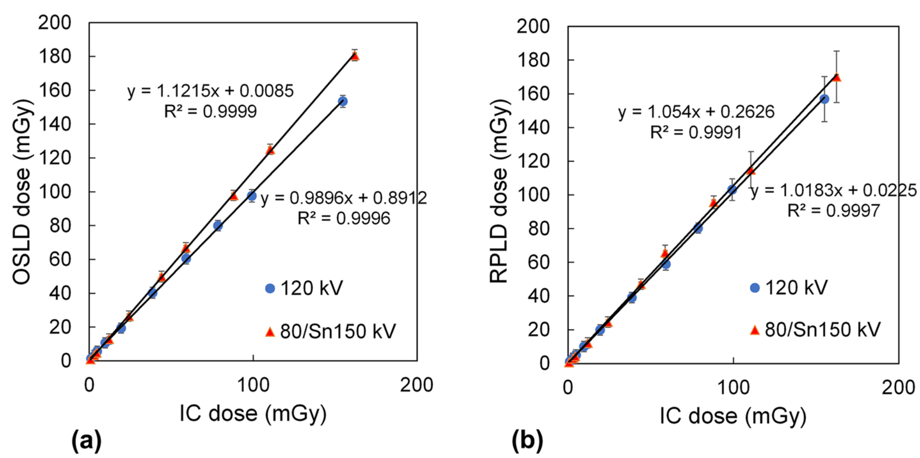

Fig. 5 Linearity of the dose response. **a** OSLD. **b** RPLD

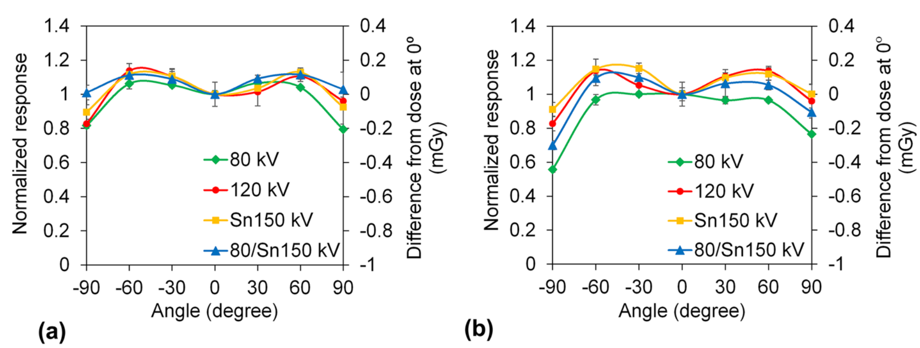

Fig. 6 Angular dependence normalized to the response at 0°. **a** OSLD. **b** RPLD

RPLD in the SE mode ranged from 0.80 ± 0.00 to 1.14 ± 0.04 and from 0.56 ± 0.02 to 1.15 ± 0.03 and those for the OSLD and RPLD in the DE mode ranged from 1.00 ± 0.02 to 1.12 ± 0.03 and from 0.70 ± 0.03 to 1.11 ± 0.04, respectively. For the OSLD, the influence of tube voltage on the normalized dose response was small, and the normalized dose responses were higher at ± 30° and ± 60° in SE and DE modes, and lower at ± 90° in only SE mode. The value at − 90° were 0.82 ± 0.02, 0.83 ± 0.03, and 0.90 ± 0.04 for 80, 120, and Sn150 kV, respectively, while those at + 90° were 0.80 ± 0.00, 0.96 ± 0.02, and 0.92 ± 0.01 for 80, 120, and Sn150 kV, respectively. However, the normalized responses at both − 90° and + 90° were larger than that at 0° in the DE mode. Conversely, as the tube voltage decreased, the difference of normalized dose response for the RPLD was larger in the SE mode. Also, the normalized response of the RPLD was higher at ± 30° and ± 60°, and markedly lower at − 90° at 120 and Sn150 kV and DE modes. The values at − 90° was 0.56 ± 0.02, 0.83 ± 0.04, 0.91 ± 0.04, and 0.70 ± 0.03 for 80, 120, and Sn150 kV, and the DE mode, respectively. These values were smaller when compared to the response at 90°. Further, the difference of the normalized dose response for the OSLD was smaller than that for the RPLD.

Discussion

In this study, we evaluated the properties of OSLD and RPLD for dual-source DECT dosimetry considering energy dependence, dose variation, dose linearity, and angular dependence. The relative dose response compared to the ionization chamber decreased by 3.8% with the OSLD and 6.6% with the RPLD when compared with those observed for SE under equivalent effective energy. The dose variation for the OSLD and RPLD in the DE mode were 1.8% and 2.6%, respectively. There was a linear relationship between the dose measured using the dosimeter and that measured by the ionization chamber in the DE mode with involvement of both the OSLD and RPLD. In the DE mode, the normalized response of OSLD was higher at − 90° and + 90°. Also, the normalized response of the RPLD was higher at ± 30° and ± 60°, and markedly lower at − 90°.

The difference of the HVLs was small regardless of the combination of low and high tube voltages in the DE mode. We used the preset ratio of the tube current adjusted by Siemens Healthineers. While the HVLs and effective energies are influenced by the ratio of tube currents from both tubes, the ratios of the tube current from tube A and tube B depended upon the combination of low and high tube voltages. The differences of the relative dose response for OSLD and RPLD were small regardless of the combination of low and high tube voltages in the DE mode. Previous study showed that the energy dependence of OSLD was smaller than that of RPLD in single energy [12, 14, 21], and this study indicated that the energy dependence of OSLD was smaller than that of RPLD in SE mode and the energy dependence both OSLD and RPLD were small in DE mode. The results of DE mode reflected that the difference of the HVLs was small regardless of the combination of low and high tube voltages. The relative dose responses of the OSLD and RPLD in the DE mode decreased by 3.8% and 6.6% when compared with those for the SE mode, which was under equivalent effective energy. There can be more than one shape of the X-ray spectrum, even if the effective energy is equivalent [22]. The relative dose responses both OSLD and RPLD were lower when X-ray of higher energy levels were irradiated according to the result of SE mode. The relative response of DE mode was lower than that of SE mode because the X-ray spectrum of DE mode contained high energy. The difference in relative dose response of the RPLD was larger than that for the OSLD when X-ray of higher energy levels were irradiated, therefore, the difference in relative dose response between the SE and DE modes was larger for the RPLD than for the OSLD. When OSLDs and RPLDs are used for dose measurement in DECT, the same calibration factor with SE mode should not be adopted.

Previous study showed that the dose variation of OSLD was 1.5–3.3% and that of RPLD was 2.8% in single energy [12, 14, 21], this study indicated that the average coefficient of dose variation for both the OSLD and the RPLD were within 3% regardless of tube voltages. The dose variation of the OSLD and RPLD in the SE mode were comparable to those in the DE mode, so it is suggested that the influence of dose variation in the DE mode is small.

In the OSLD and RPLD, there was a linear relationship observed between the dose measured by the dosimeter and that measured by the ionization chamber for both the SE and DE modes within the range of 1 to 150 mGy. The correlation coefficients were similar to those seen in previous studies for thermoluminescent dosimeters [23, 24]. Yusuf et al. [13] reported that the correction factor between the ionization chamber and the OSLD at 80 kV X-ray was 0.9899 when investigating the linearity for OSLD response. Sato et al. [25] observed that the RPLD had satisfactory linearity in a dose range of 10 to 10^4 mGy. Manninen et al. [26] found that the RPLD showed excellent linearity with a filter in the 20 μGy to 11 mGy dose range and without a filter in the 2 to 10 Gy range, the correlation coefficients were 0.999. These results indicate that both the OSLD and RPLD have linear relationship with the ionization chamber from low to high dose regardless of tube voltage in the SE mode. Our results suggested that the OSLD and RPLD have linear relationship with the ionization chamber not only in the SE mode but also the DE mode. The slope of the approximation curve for dose response between the OSLD and the ionization chamber in DE mode was larger than that in 120 kV. The normalized dose response for DE mode was higher than that for SE modes regardless of the irradiation angle in OSLD (Fig. 6), and it affected the slope of the approximation curve for dose response between the OSLD and the ionization chamber.

Al-Senan and Hatab [21] recorded dose reductions of 18% and 5% at + 90° with 80 and 120 kV, respectively, when using the OSLD. In the present study, the decrease of response at + 90° was consistent with their reports. The decrease of response at + 90° was attributed to the shaping of the plastic case and hardening of the beam by the sensitive volume of the OSLD itself [21]. A previous study found the angular dependence of the OSLD is also energy-dependent [21], however, the influence of energy was small within the energy range used in the present study. In particular, the difference of normalized dose response of the OSLD in the DE mode was smaller than that in the SE mode, because the influence of dose reduction on the OSLD for the horizontal direction was small regardless of tube voltage. It appears that the angular dependence of the RPLD was also energy-dependent, but it was equivalent between SE and DE modes in the present study. Hirosawa et al. [14] noted that the dose response decreased when X-ray was irradiated at – 90°. The decrease in dose response is believed to be due to the cylindrical shape of the RPLD. When X-ray is irradiated parallel to the long axis of the rod, it is more significantly absorbed by glass of RPLD. In comparing the results of angular dependence for the OSLD and RPLD, the difference of the normalized dose response when using the OSLD was smaller than that seen when using the RPLD because the energy dependence of the OSLD was smaller than that of the RPLD.

Our results lead us to summarize the following: (1) For the OSLD, the influence of the tube voltage combination and irradiation angle on relative dose response is smaller in the DE mode than in the SE mode, and dose variation and dose linearity were equivalent between the SE and DE modes. (2) For the RPLD, the influence of the tube voltage combination was smaller in the DE mode than in the SE mode, and angular dependence, dose variation, and dose linearity were equivalent between the SE and DE modes. The decrease of the response at 90° in DE mode was as large as that in SE mode. (3) For the OSLD and RPLD, the relative dose responses of DE mode did not coincide those of SE mode under equivalent effective energy. Therefore, our findings revealed both OSLD and RPLD can perform dual-source DECT dosimetry similar to SECT dosimetry after calibrating by DECT X-ray beam quality. However, angular dependence of RPLD would influence for DECT dosimetry when X-ray is irradiated parallel along the long direction of it.

This study had some limitations that should be considered. Firstly, TLDs, which have been used for a long time as passive radiation detection devices for dose monitoring or to measure the dose affecting the patient, were not assessed in this study. Secondly, this study did not use reference beams in a metrological facility, instead employing beams irradiated from a clinical dual-source CT scanner. To evaluate the detailed characteristics of OSLDs and RPLDs such as dose variation and angle and energy response, it should be considered to perform some tests with irradiation in a metrological facility in a future study.

Conclusion

We evaluated the properties of the OSLD and RPLD for dose measurement in dual-source DECT in terms of energy dependence, dose variation, dose linearity, and angular dependence. For both the OSLD and RPLD, the influence of these properties in DE mode was equal or smaller than those in SE mode, and the relative dose responses of DE mode did not coincide those of SE mode under equivalent effective energy. Therefore, both OSLD and RPLD can performed dual-source DECT dosimetry similar to SECT dosimetry after calibrating by DECT X-ray beam quality. However, angular dependence of RPLD would influence for DECT dosimetry when X-ray is irradiated parallel along the long direction of it.

Acknowledgements We would like to express our gratitude to Mr. Hiroshi Takamatsu of Siemens Healthineers Japan and Mr. Yasuhiro Hirano of Marubun Tsusho, who provided technical assistance with the experiments.

Funding This work was supported by JSPS KAKENHI Grant Number JP18K07746.

Declarations

Conflict of interest The authors declare no conflicts of interest exist.

Ethical approval Not applicable. This article does not contain any studies with human participants or animals performed by any of the authors.

References

1. Regulla DF, Eder H (2005) Patient exposure in medical X-ray imaging in Europe. Radiat Prot Dosim 114:11–25
2. Kang MJ, Park CM, Lee CH et al (2010) Dual-energy CT: clinical applications in various pulmonary diseases. Radiographics 30:685–698
3. Lee KYG, Cheng HMJ, Chu CWA et al (2019) Metal artifact reduction by monoenergetic extrapolation of dual-energy CT in patients with metallic implants. J Orthop Surg 27:1–7
4. Long Z, Bruesewitz MR, DeLone DR et al (2018) Evaluation of projection- and dual-energy-based methods for metal artifact reduction in CT using a phantom study. J Appl Clin Med Phys 19:252–260

5. International Commission of Radiological Protection (2000) Managing patient dose in computed tomography. Ann ICRP 30:7–45
6. Giansante L, Martins JC, Nersissian DY et al (2019) Organ doses evaluation for chest computed tomography procedures with TL dosimeters: comparison with Monte Carlo simulations. J Appl Med Phys 20:308–320
7. Moore WH, Bonvento M, Olivieri-Fitt R (2006) Comparison of MDCT radiation dose: a phantom study. AJR Am J Roentgenol 187:498–502
8. Diekmann S, Siebert E, Juran E et al (2010) Dose exposure of patients undergoing comprehensive stroke imaging by multidetector-row CT: comparison of 320-detector row and 64-detector row CT scanners. AJRNR Am Neuroradiol 31:1003–1009
9. Zhang D, Li X, Gao Y et al (2013) A method to acquire CT organ dose map using OSL dosimeters and ATOM anthropomorphic phantoms. Med Phys 40:081918
10. Paul AJ (2007) Characterization of optically stimulated luminescent dosimeters, OSLDs, for clinical dosimetric measurements. Med Phys 34:4594–4604
11. Kadoya N, Shimomura K, Kitou S et al (2012) Dosimetric properties of radiophotoluminescent glass detector in low-energy photon beams. Med Phys 39:5910–5916
12. Scarboro SB, Cody D, Alvarez P et al (2015) Characterization of the nanodot OSLD dosimeter in CT. Med Phys 42:1797–1807
13. Yusuf M, Saoudi A, Alothmany N et al (2014) Characterization of the optically stimulated luminescence nanoDot for CT dosimetry. Life Sci J 11:445–450
14. Hirosawa A, Matsubara K, Kondo H et al (2015) Properties and usage of radiophotoluminescent glass dosimeters for computed tomography dosimetry. Nihon Hoshasen Gijutsu Gakkai Zasshi 71:12–18 (**in Japanese**)
15. Scarboro SB, Kry SF (2012) Characterisation of energy response of Al_2O_3: C optically stimulated luminescent dosimeters (OSLDs) using cavity theory. Radiat Prot Dosim 153:23–31
16. Hill R, Mo Z, Haque M et al (2009) An evaluation chambers for the relative dosimetry of kilovoltage X-ray beams. Phys Med 36:3971–3981
17. Yahnke C (2009) Calibrating the microStar. Landauer, Glenwood
18. International Organization for Standization (2008) Guide to the expression of uncertainties in measurement. ISO 98–3
19. Matsubara K, Ichikawa K, Murasaki Y et al (2014) Accuracy of measuring half- and quarter- value layers and appropriate aperture width of a convenient method using a lead-covered case in X-ray computed tomography. J Appl Clin Med Phys 15:309–316
20. Seltzer SM, Hubbell JH (1996) Tables and graphs of photon mass attenuation coefficients and mass energy-absorption coefficients for photon energies 1 keV to 20 MeV for elements Z=1 to 92. The X-ray Attenuation and Absorption for Materials of Dosimetric Interest Database. NIST. https://doi.org/10.18434/T4D01F
21. Al-Senan RM, Hatab MR (2011) Characteristics of an OSLD in the diagnostic energy range. Med Phys 38:4396–4405
22. Kato H, Hayashi N, Suzuki S et al (2011) Problem of the effective energy used as a quality expression of diagnostic X-ray. Nihon Hoshasen Gijutsu Gakkai Zasshi 67:1320–1326
23. Carvalho Junior AB, Barros TF, Guzzo PL et al (2012) Manufacturing polycrystalline pellets of natural quartz for applications in thermoluminescence dosimetry. Mater Res 15:536–543
24. Hsu SM, Lai YC, Jeng CC et al (2017) Dosimetric comparison of different treatment modalities for stereotactic radiotherapy. Radiat Oncol 12:155
25. Sato F, Zush N, Nagai T et al (2013) Development of radiophotoluminescence glass dosimeter usable in high temperature environment. Radiat Meas 53–54:8–11
26. Manninen AL, Koivula A, Nieminen MT (2012) The applicability of radiophotoluminescence dosimeter (RPLD) for measuring medical radiation (MR) doses. Radiat Prot Dosim 151:1–9